Plasmon-Modulated Light Scattering from Gold Nanocrystal-Decorated Hollow Mesoporous Silica Microspheres

*Manda Xiao, Huanjun Chen, Tian Ming, Lei Shao, and Jianfang Wang**

Department of Physics, The Chinese University of Hong Kong, Shatin, Hong Kong SAR, China

Supporting Information

(1) Calculation of the Scattering Spectra of the HMSMSs by Mie Theory

Mie theory is utilized to calculate the scattering spectra of the HMSMSs that are not coated with Au nanocrystals. Specifically, Mie theory extended to core–multishell structures on the basis of the recursion algorithm is employed.[1,2] An individual HMSMS is modeled as a spherical core–shell structure embedded in water. The hollow core is filled with water with a refractive index of 1.33. The index of the mesoporous silica shell is estimated to be 1.39 according to the pore volume of the silica shell. The average diameter of the core and thickness of the shell measured from the SEM and TEM imaging are employed. The summation coefficients for calculating the scattering and absorption cross sections and electromagnetic field distributions can be obtained from the expressions below[1]

$$T_n^1 = -\frac{m_1\psi_n(m_1y_1)\psi_n'(y_1) - \psi_n'(m_1y_1)\psi_n(y_1)}{m_1\chi_n(m_1y_1)\psi_n'(y_1) - \chi_n'(m_1y_1)\psi_n(y_1)} \tag{1}$$

$$T_n^s = -\frac{m_s\psi_n(m_sy_s)\left[\psi_n'(y_s) + T_n^{s-1}\chi_n'(y_s)\right] - \psi_n'(m_sy_s)\left[\psi_n(y_s) + T_n^{s-1}\chi_n(y_s)\right]}{m_s\chi_n(m_sy_s)\left[\psi_n'(y_s) + T_n^{s-1}\chi_n'(y_s)\right] - \chi_n'(m_sy_s)\left[\psi_n(y_s) + T_n^{s-1}\chi_n(y_s)\right]} \tag{2}$$

$$a_n = -\frac{m_r\psi_n(m_ry_r)\left[\psi_n'(y_r) + T_n^{r-1}\chi_n'(y_r)\right] - \psi_n'(m_ry_r)\left[\psi_n(y_r) + T_n^{r-1}\chi_n(y_r)\right]}{m_r\xi_n(m_ry_r)\left[\psi_n'(y_r) + T_n^{r-1}\chi_n'(y_r)\right] - \xi_n'(m_ry_r)\left[\psi_n(y_r) + T_n^{r-1}\chi_n(y_r)\right]} \tag{3}$$

$$S_n^1 = -\frac{\psi_n(m_1y_1)\psi_n'(y_1) - m_1\psi_n'(m_1y_1)\psi_n(y_1)}{\chi_n(m_1y_1)\psi_n'(y_1) - m_1\chi_n'(m_1y_1)\psi_n(y_1)} \tag{4}$$

$$S_n^s = -\frac{\psi_n(m_s y_s)\left[\psi_n'(y_s) + S_n^{s-1}\chi_n'(y_s)\right] - m_s\psi_n'(m_s y_s)\left[\psi_n(y_s) + S_n^{s-1}\chi_n(y_s)\right]}{\chi_n(m_s y_s)\left[\psi_n'(y_s) + S_n^{s-1}\chi_n'(y_s)\right] - m_s\chi_n'(m_s y_s)\left[\psi_n(y_s) + S_n^{s-1}\chi_n(y_s)\right]} \quad (5)$$

$$b_n = -\frac{\psi_n(m_r y_r)\left[\psi_n'(y_r) + S_n^{r-1}\chi_n'(y_r)\right] - m_r\psi_n'(m_r y_r)\left[\psi_n(y_r) + S_n^{r-1}\chi_n(y_r)\right]}{\xi_n(m_r y_r)\left[\psi_n'(y_r) + S_n^{r-1}\chi_n'(y_r)\right] - m_r\xi_n'(m_r y_r)\left[\psi_n(y_r) + S_n^{r-1}\chi_n(y_r)\right]} \quad (6)$$

In the above equations, the parameter s is the shell index of the structure, with s = 1 representing the core and s = 2 standing for the shell. The parameter r denotes the index of the outmost shell. For our HMSMSs, r = 3 stands for the surrounding water. The parameters $m_s = n_{s+1}/n_s$ represent the refractive index ratio between the s + 1 shell and s shell. The wavenumber in each shell is $k_s = (2\pi n_s)/\lambda$, with λ being the wavelength of light in vacuum. The Riccati-Bessel functions are defined as

$$\psi_n(y_s) = y_s j_n(y_s) \quad (7)$$

$$\chi_n(y_s) = y_s y_n(y_s) \quad (8)$$

$$\xi_n(y_s) = y_s h_n^{(1)}(y_s) \quad (9)$$

where $h_n^{(1)}(y_s)$ is the Hankel function of the first kind. The prime denotes the derivation of the function with respect to its argument. $y_s = k_s R_s$, with R_s being the radius of each shell. After the coefficients a_n and b_n are calculated, the electromagnetic field distributions at a specific distance R_0 outside the core–shell sphere can be obtained as

$$E_{s\theta} = \frac{\cos\phi}{\rho}\sum_{n=1}^{\infty} E_n\left(-ia_n\xi_n'\tau_n + b_n\xi_n\pi_n\right) \quad (10)$$

$$E_{s\phi} = \frac{\sin\phi}{\rho}\sum_{n=1}^{\infty} E_n\left(-b_n\xi_n\tau_n + ia_n\xi_n'\pi_n\right) \quad (11)$$

$$H_{s\theta} = \frac{k_r}{\omega\mu}\frac{\sin\phi}{\rho}\sum_{n=1}^{\infty} E_n\left(-ib_n\xi_n'\tau_n + a_n\xi_n\pi_n\right) \quad (12)$$

$$H_{s\phi} = \frac{k}{\omega\mu}\frac{\cos\phi}{\rho}\sum_{n=1}^{\infty} E_n\left(-ib_n\xi_n'\pi_n + a_n\xi_n\tau_n\right) \quad (13)$$

$$E_n = i^n E_0 \frac{2n+1}{n(n+1)} \tag{14}$$

where $\rho = k_r R_0$, π_n, τ_n are the functions defined previously,[2] and E_0 is the magnitude of the incident electric field. In practical calculations, a truncation of n can be applied according to the following criterion[3]

$$n_{\max} = y_r + 4.05 y_r^{\frac{1}{3}} + 2 \tag{15}$$

Once the above electromagnetic fields are calculated, the scattered power and therefore the scattering spectrum inside a solid angle towards a specific direction can be obtained from

$$W_s = \frac{1}{2} \mathrm{Re} \int_{\varphi_1}^{\varphi_2} \int_{\theta_1}^{\theta_2} \left(E_{s\theta} H_{s\varphi}^* - E_{s\varphi} H_{s\theta}^* \right) R_0^2 \sin\theta d\theta d\varphi \tag{16}$$

In our calculations, the integration range of θ and φ are determined by the dark-field scattering geometry of our optical system, which is shown in Figure S5. Incident light with linear polarization is considered in our calculations. From the numerical aperture (NA = 0.5) of the dark-field objective, we can determine that $\theta_1 = 115°$, $\theta_2 = 175°$, $\varphi_1 = 60°$, and $\varphi_2 = 120°$.

REFERENCES

(1) Sinzig, J.; Quinten, M. *Appl. Phys. A* **1994**, *58*, 157–162.

(2) Bohren, C.; Huffman, D. *Absorption and Scattering of Light by Small Particles*; New York: Wiley, 1983.

(3) Barber, P. W.; Hill, S. C. *Light Scattering by Particles: Computational Methods*; Singapore: World Scientific Publishing, 1990.

(2) Calculation of the Scattering, Absorption, and Extinction Spectra of the Au Nanocrystals

Finite-difference time-domain (FDTD) method was used to calculate the scattering, absorption, and extinction spectra of the Au nanocrystals. The FDTD method is an explicit time marching algorithm

used to solve Maxwell's curl equations on a discretized spatial grid. It can be used to study both the near- and far-field electromagnetic responses of metal nanoparticles of arbitrary shapes. We employed a software package, FDTD Solutions, developed by Lumerical Solutions, Inc., for our calculations. The Au dielectric function was represented using the Drude model, with parameters chosen to match the bulk gold dielectric data. In our FDTD calculations, a nanocrystal was surrounded by a virtual boundary with an appropriate size. The Au nanocrystal and its surrounding medium inside the boundary were divided into meshes of 0.5 nm in size. An electromagnetic pulse was launched into the boundary to simulate a propagating plane wave interacting with the nanocrystal. For the Au nanorods, only the longitudinal plasmon resonance mode was calculated by setting the electric field of the plane wave parallel to the length direction of the nanorod. In the calculations, the surrounding medium of the Au nanocrystals was set to be water with a refractive index of 1.33. The sizes of the Au nanocrystals were taken to match their average values. The Au nanosphere was modeled as a perfect sphere. The nanorod was modeled as a cylinder capped with two half-spheres at the ends. The small differences between the calculated plasmon wavelengths and the measured ones can be ascribed to the measurement errors in the nanocrystal sizes.

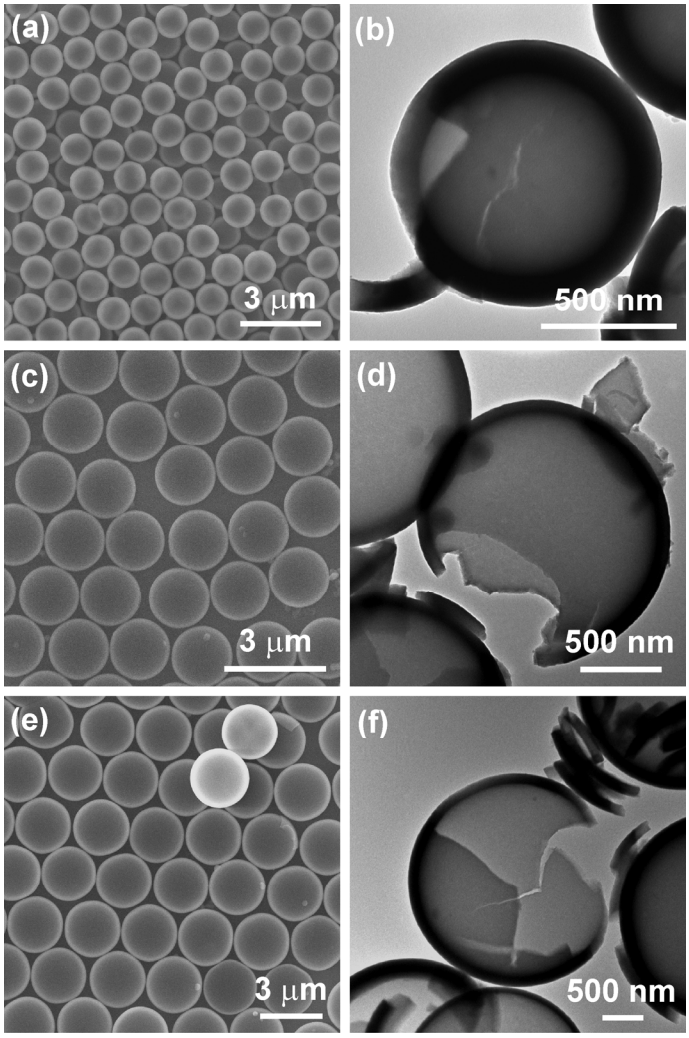

Figure S1. (a, c, e) SEM images of the three HMSMS samples, respectively. (b, d, f) TEM images of the three samples, respectively. The samples were crushed deliberately so that the shell thickness could be measured. The average outer diameters/shell thicknesses of the three samples were measured to be 1.22 ± 0.04 μm/108 ± 3 nm, 1.80 ± 0.02 μm/77 ± 4 nm, and 2.72 ± 0.04 μm/134 ± 6 nm from top to bottom, respectively.

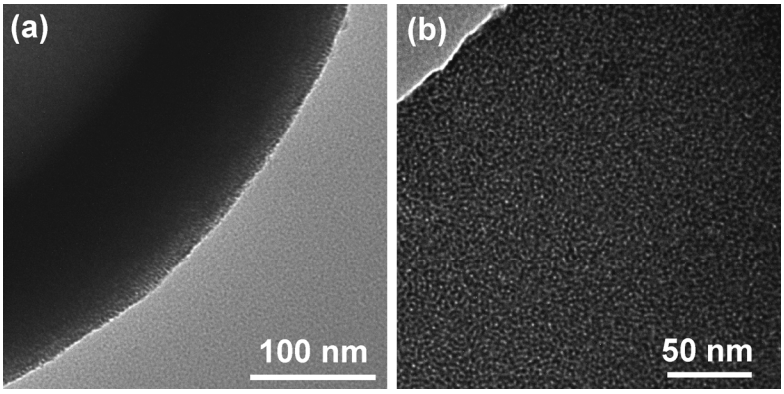

Figure S2. TEM images showing the porous structure of the HMSMSs: (a) the edge of an HMSMS, (b) a piece of the crushed HMSMSs. The imaged HMSMS sample has an average outer diameter of 1.22 μm.

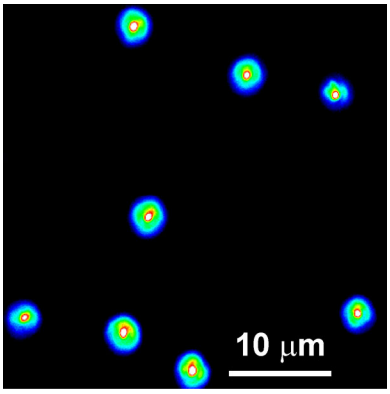

Figure S3. Representative dark-field scattering image of the spatially-isolated HMSMSs. The average diameter of the HMSMS sample is 1.80 μm.

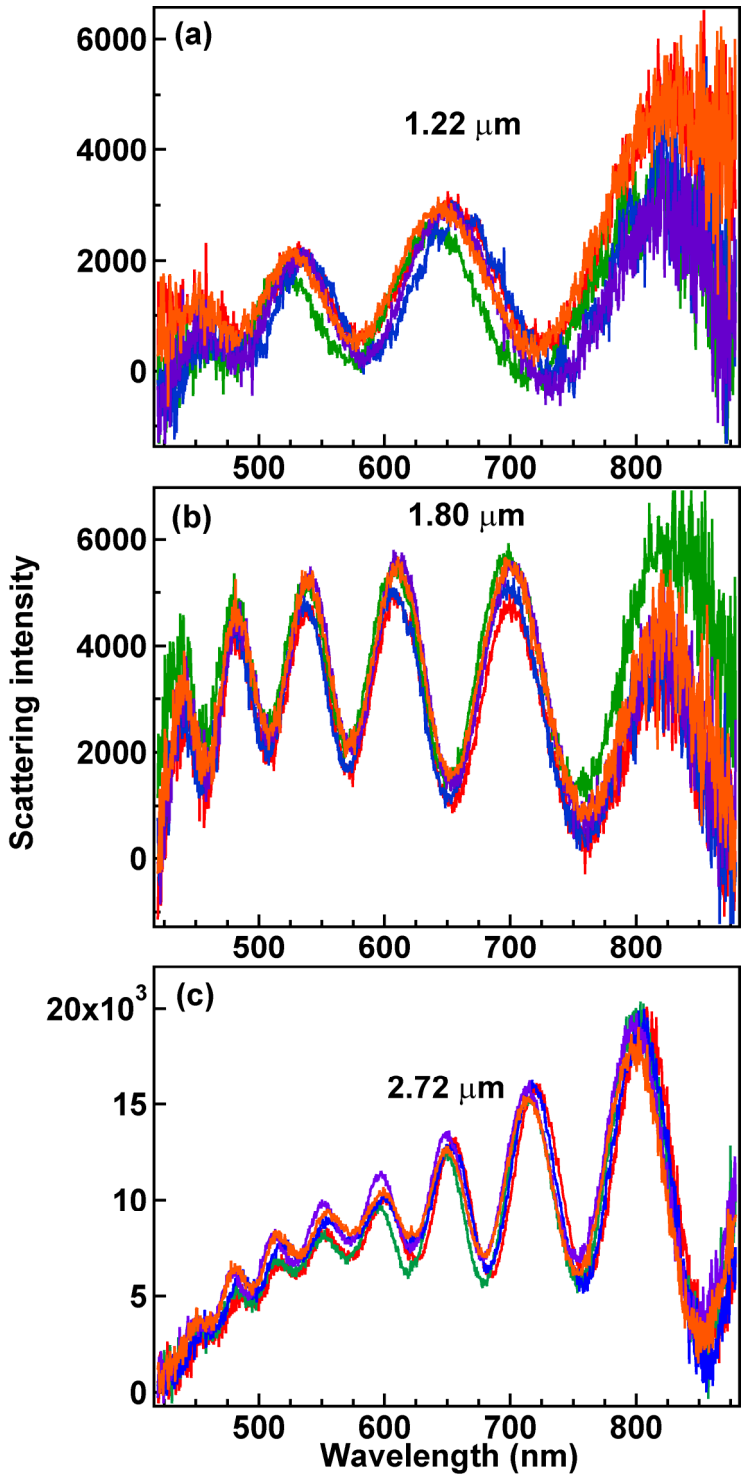

Figure S4. Representative scattering spectra recorded from the individual HMSMSs: (a) 1.22-μm HMSMSs, (b) 1.80-μm HMSMSs, (c) 2.72-μm HMSMSs. Five spectra are plotted together for each sample. The scattering spectra taken from the different microspheres for the same HMSMS sample nearly overlap with each other, showing the high size uniformity of the HMSMS samples.

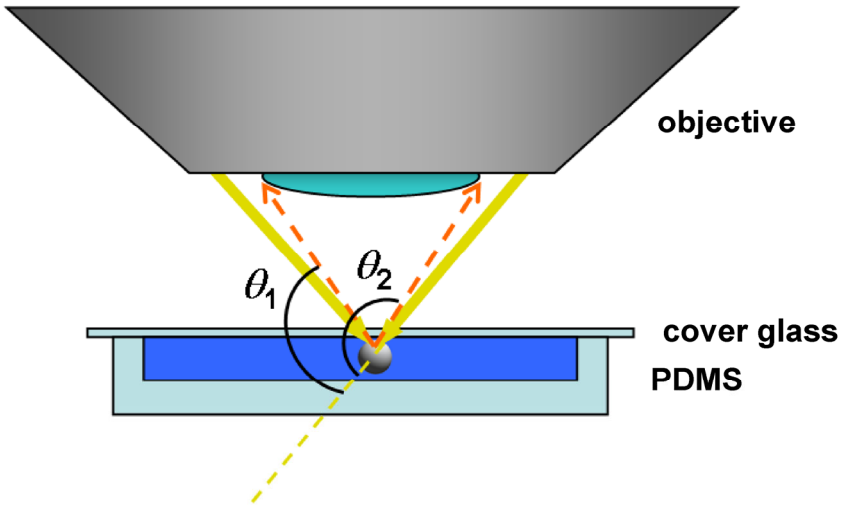

Figure S5. Schematic showing the geometric configuration of the dark-field scattering technique.

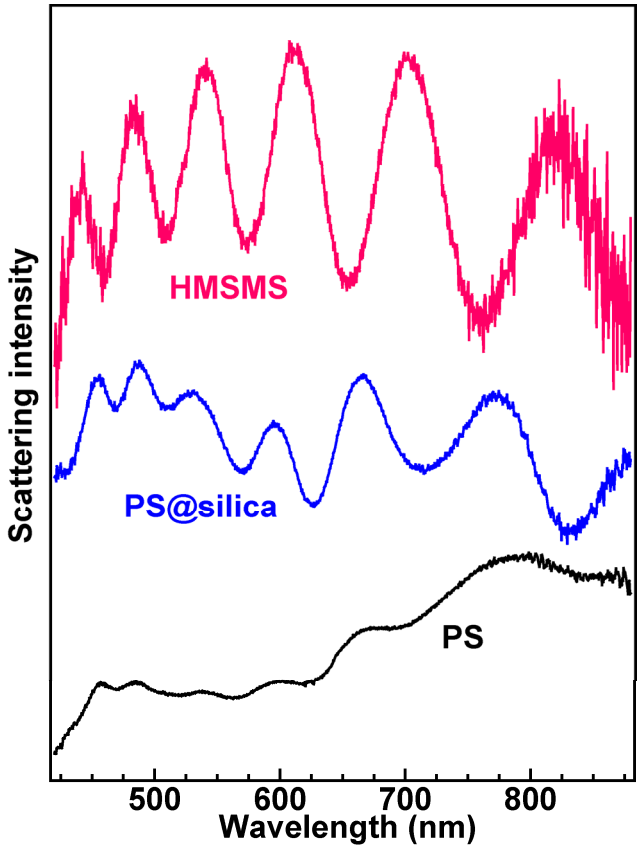

Figure S6. Comparison of the typical scattering spectra acquired from the individual polystyrene microspheres, silica-coated polystyrene microspheres, and HMSMSs, respectively. The average

diameter of the polystyrene microsphere sample is 1.73 μm, and the average outer diameter of the HMSMS sample is 1.80 μm. The spectra have been shifted vertically for clarity.

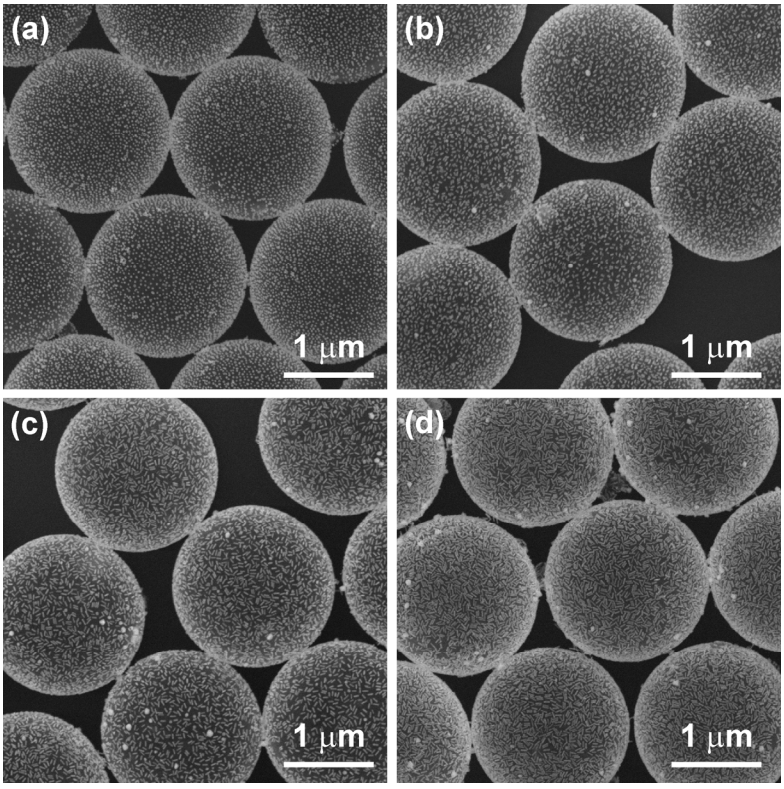

Figure S7. SEM images of the 1.80-μm HMSMSs coated with the Au nanocrystals that have SPRWs of (a) 526 nm, (b) 622 nm, (c) 756 nm, and (d) 853 nm, respectively.

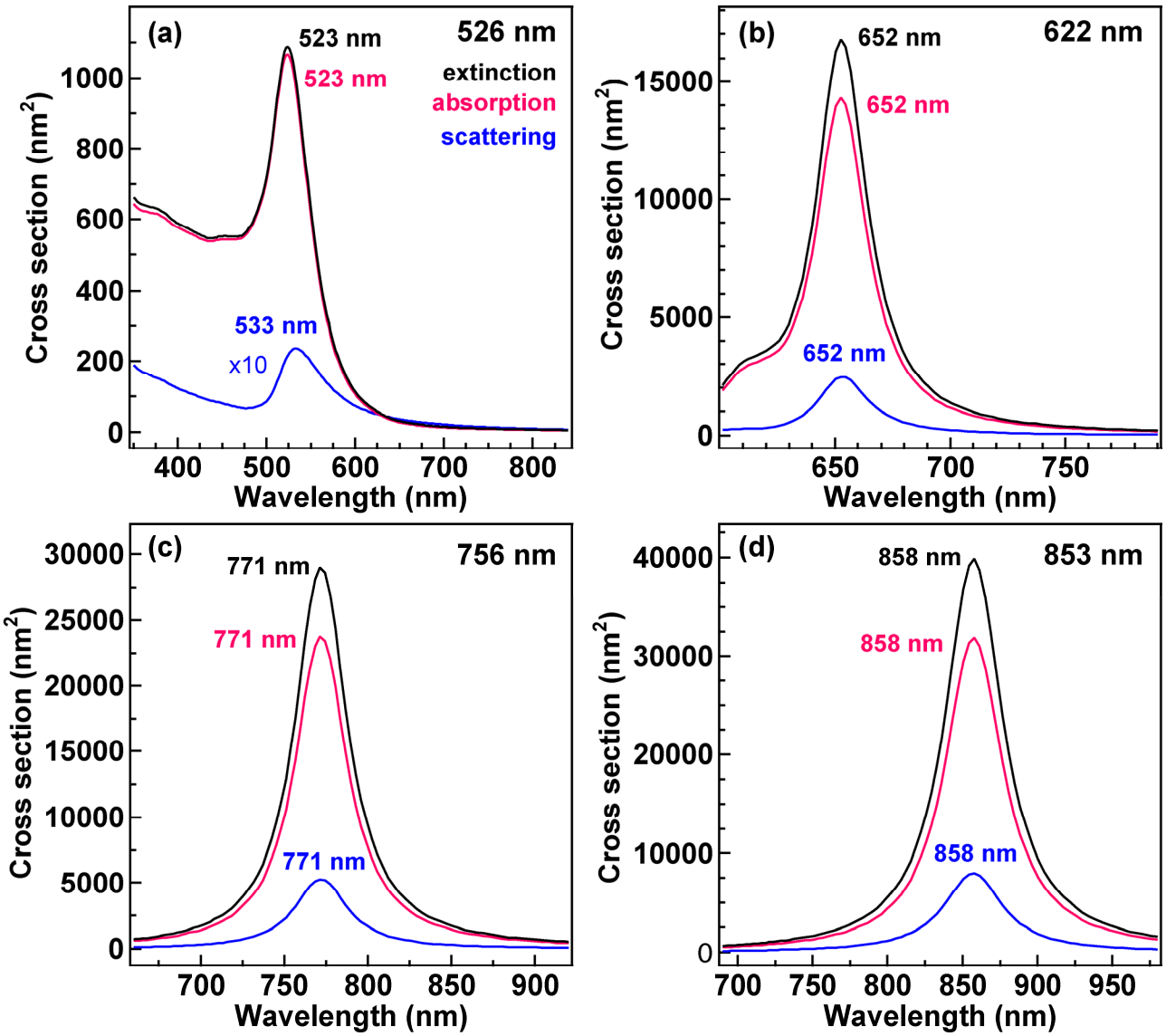

Figure S8. Scattering (blue), absorption (red), and extinction (black) spectra of the Au nanocrystals obtained from the FDTD calculations. (a) The Au nanosphere sample with an ensemble plasmon wavelength of 526 nm. The scattering spectrum has been multiplied by 10. (b) The Au nanorod sample with an ensemble longitudinal plasmon wavelength of 622 nm. (c) The Au nanorod sample with an ensemble longitudinal plasmon wavelength of 756 nm. (d) The Au nanorod sample with an ensemble longitudinal plasmon wavelength of 853 nm.

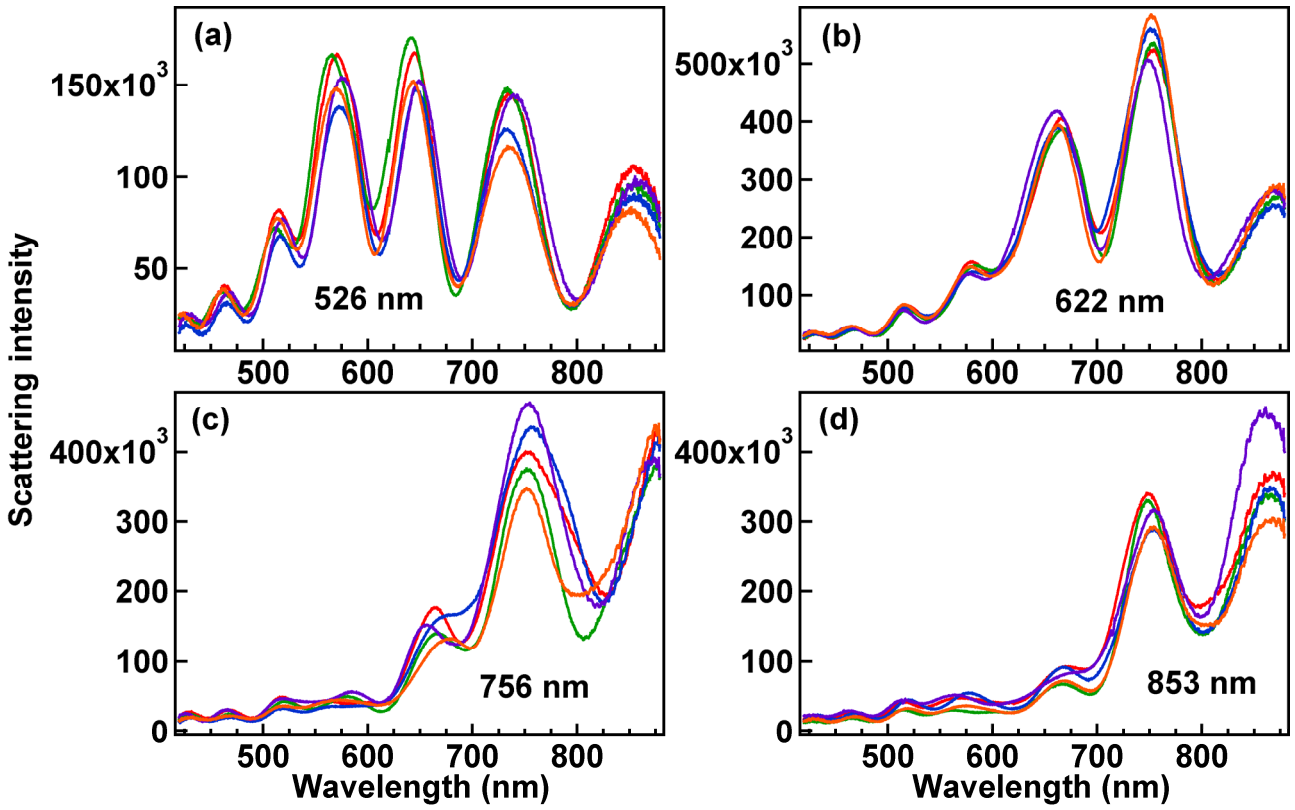

Figure S9. Representative scattering spectra taken from the individual 1.80-μm HMSMSs coated with the differently-sized Au nanocrystals, respectively. The number in each plot is the SPRW of the Au nanocrystals: (a) 526 nm, (b) 622 nm, (c) 756 nm, and (d) 853 nm. Five spectra are plotted together for each sample. The scattering spectra acquired from the different microspheres for the same sample nearly overlap with each other, suggesting the high uniformity of the coating of the Au nanocrystals on the HMSMSs.

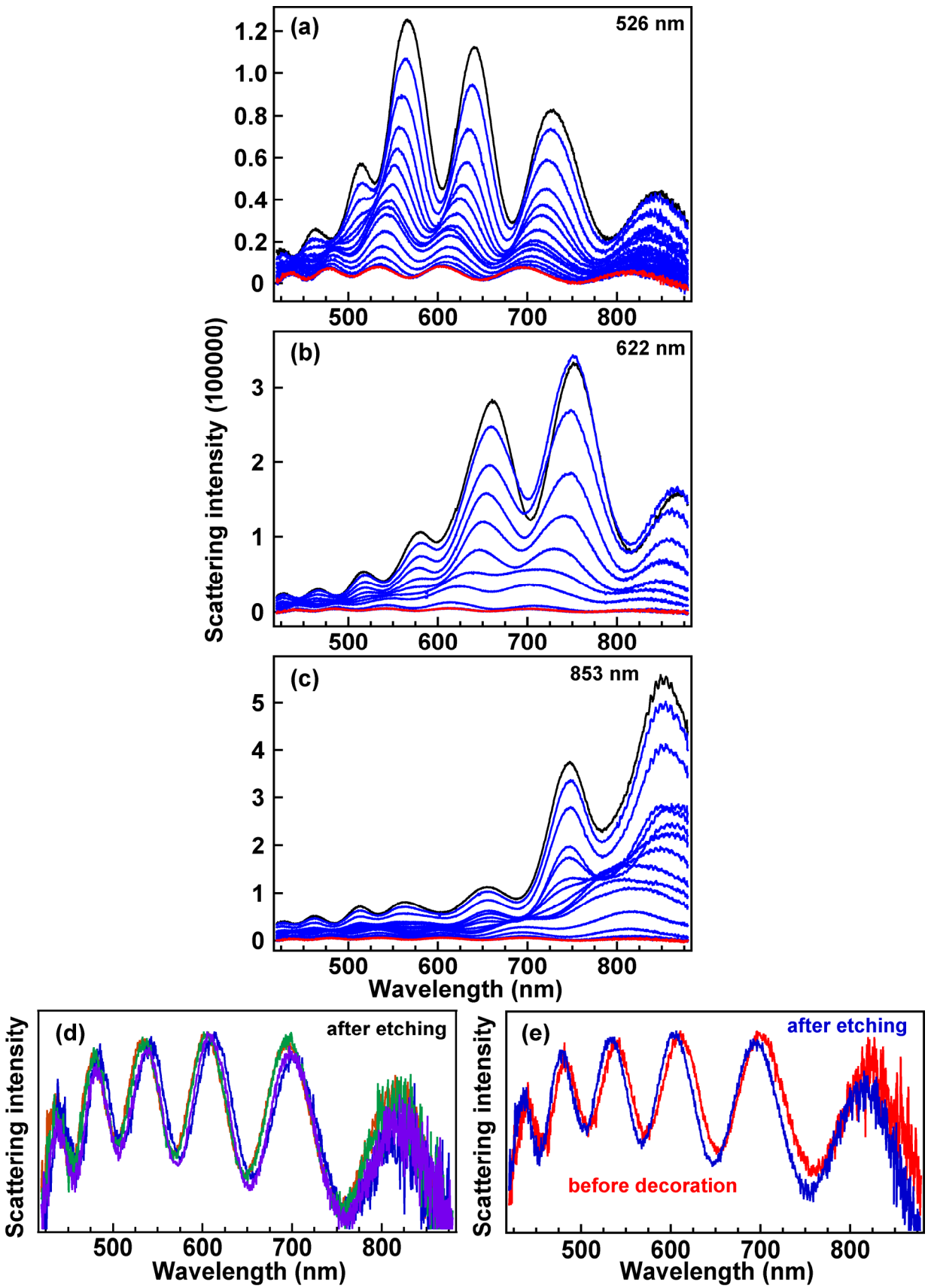
(a)
526 nm
(b)
622 nm
(c)
853 nm
Scattering intensity (100000)
Wavelength (nm)
(d)
after etching
Scattering intensity
Wavelength (nm)
(e)
after etching
before decoration
Scattering intensity
Wavelength (nm)

Figure S10. Evolution of the scattering spectra of the individual HMSMSs decorated with the Au nanocrystals during the chemical etching process. (a) HMSMSs decorated with the Au nanospheres that have an ensemble SPRW of 526 nm. (b) HMSMSs decorated with the Au nanorods that have an ensemble longitudinal SPRW of 622 nm. (c) HMSMSs decorated with the Au nanorods that have an ensemble longitudinal SPRW of 853 nm. The average diameter of the HMSMS sample is 1.80 μm. The scattering spectra were recorded every 10 min during the chemical etching process. The black and red curves indicate the scattering spectra recorded before and after the etching, respectively. (d) Normalized scattering spectra of the HMSMSs recorded after the adsorbed Au nanocrystals were completely etched away. The graph was generated by re-plotting together the four spectra recorded after the chemical etching for the HMSMSs decorated with the four Au nanocrystal samples. (e) Comparison of the scattering spectra acquired before the decoration of the Au nanocrystals and after the complete etching of the adsorbed Au nanocrystals.